



STRUCTURAL SCIENCE  
CRYSTAL ENGINEERING  
MATERIALS

**Volume 72 (2016)**

**Supporting information for article:**

**(3+1)-incommensurately modulated crystal structure of  
Cs<sub>3</sub>ScSi<sub>6</sub>O<sub>15</sub>**

**Clivia Hejny, Volker Kahlenberg, Daniela Schmidmair and Predrag Dabić**

## (3+1) incommensurately modulated crystal structure of Cs<sub>3</sub>ScSi<sub>6</sub>O<sub>15</sub>

Clivia Hejny<sup>a\*</sup>, Volker Kahlenberg<sup>a</sup>, Daniela Schmidmair<sup>a</sup>, Martina Tribus<sup>a</sup> and Predrag Dabić<sup>b</sup>

<sup>a</sup>Institute of Mineralogy and Petrography, University of Innsbruck, Innrain 52, Innsbruck, A-6020, Austria

<sup>b</sup>Laboratory of Crystallography, University of Belgrade, Dušina 7, Belgrade, 11000, Serbia

Correspondence email: Clivia.Hejny@uibk.ac.at

### S1. Abstract

**Abstract** Single-crystal X-ray diffraction of Cs<sub>3</sub>ScSi<sub>6</sub>O<sub>15</sub> shows the presence of main reflections and satellite reflections up to the fourth order along the **c**\* direction. The (3+1)-dimensional incommensurately modulated structure was solved in superspace group  $R\bar{3}m1(00g)0s0$  [ $a = 13.861(1)$ ,  $c = 6.992(1)$  Å,  $V = 1163.4(2)$  Å<sup>3</sup>] with a modulation wavevector  $\mathbf{q} = 0.14153(2) \cdot \mathbf{c}^*$ . Refinement of three modulation waves for positional and ADP values for all atoms converged to *Ro* values for all, main and satellite reflections of first, second and third order of 0.0200, 0.0166, 0.0181, 0.0214 and 0.0303, respectively. Cs<sub>3</sub>ScSi<sub>6</sub>O<sub>15</sub> forms a mixed tetrahedral-octahedral framework with prominent six-membered rings of [SiO<sub>4</sub>]-tetrahedra interconnected by [ScO<sub>6</sub>]-octahedra. Apart from Sc all atoms are strongly affected by positional modulation with maximum atomic displacements of up to 0.93 Å causing rigid polyhedral arrangements to perform tilt- and twist movements relative to each other, such as a rotation of the Sc-octahedra around the  $\bar{3}$ -axis by over 38°. Cs has an irregular coordination environment; however, considering distances up to 3.5 Å the bond-valence sum is changing by no more than 0.02 as a function of *t* and thus overall kept at a level of ca. 1.075.

### S2. Introduction

This document contains supplementary material to the above referenced publication. The structural data can be taken from the accompanying cif file.

### S3. Raman spectroscopy

A confocal Raman spectrum was recorded in the range of 100 - 1200 cm<sup>-1</sup> with a Horiba Jobin Yvon Labram-HR 800 Raman micro-spectrometer from the same single crystal of Cs<sub>3</sub>ScSi<sub>6</sub>O<sub>15</sub> as used for the single-crystal X-ray diffraction. The sample was excited 60 seconds by using the 532 nm emission

line of a frequency-doubled 100 mW Nd:YAG laser under an Olympus 100x objective lens. The size of the laser spot on the surface was approximately 1  $\mu\text{m}$ . The scattered light was dispersed by an optical grating with 1800 lines/mm and collected by a 1024 x 256 open electrode CCD detector. Confocal pinhole and spectrometer entrance slit were set to 1000 and 100  $\mu\text{m}$ , respectively. The spectral resolution, determined by measuring the Rayleigh line, was less than 2  $\text{cm}^{-1}$ . The spectrum was recorded unpolarised. The accuracy of the Raman line shifts, calibrated by regularly measuring the Rayleigh line, was in the order of 0.5  $\text{cm}^{-1}$ . Background and Raman bands were fitted by the built-in spectrometer software LabSpec to second-order polynomial and convoluted Gaussian–Lorentzian functions, respectively.

In the Raman spectra of single-crystalline  $\text{Cs}_3\text{ScSi}_6\text{O}_{15}$  (see Figure S1) bands could be detected between 80 and 1145  $\text{cm}^{-1}$ . The spectrum can be subdivided into two regions: at low- and medium-wavenumbers up to ca. 800  $\text{cm}^{-1}$  a large number of partly overlapping bands were detected. After a gap lacking any bands from 800 to 1000  $\text{cm}^{-1}$  the most intense band of the spectrum was observed in the high-wavenumber region at 1143.3  $\text{cm}^{-1}$  next to another intense signal at 1053.2  $\text{cm}^{-1}$ .

No Raman spectra have been reported for the related structures of  $\text{Cs}_3\text{DySi}_6\text{O}_{15}$  and  $\text{Cs}_{1.86}\text{K}_{1.14}\text{DySi}_6\text{O}_{15}$  or other known alkali silicates containing ring-shaped  $[\text{Si}_6\text{O}_{18}]$ -units within a framework structure. The closest proximity can be found in Raman spectra of other mixed tetrahedral–octahedral framework structures containing three- or four-membered rings of  $[\text{SiO}_4]$ -tetrahedra with an A-1 type *PME* of identical coordination sequence up to  $k = 3$  such as wadeite-related structures (Chang et al. 2013, Hejny et al. 2012, Sitarz et al. 1997). The Raman spectra of these compounds have split spectra with a 200  $\text{cm}^{-1}$  wide gap lacking Raman-bands between the mid- and the high-wavenumber region. Comparison with these spectra allows the following conclusion: The Raman-active bands in the high-wavenumber region above 1000  $\text{cm}^{-1}$  can be assigned to Si–O–Si stretching vibrations, those in the mid-wavenumber regions of 300 – 800  $\text{cm}^{-1}$  are characteristic for the ring structures and are caused by breathing, stretching and deformation modes for the silicate ring, and bands in the low-wavenumber region are associated with translational modes of the whole ring and the non-ring cations.

#### S4. Additional figures

In the following additional figures that might help to further illustrate the topics discussed in the text are given. The reciprocal space reconstruction of the  $h0l$  layer in Figure S2 complements Figure 1. In Figures S3 – S8 electron density sections  $x_1$ - $x_4$ ,  $x_2$ - $x_4$  and  $x_3$ - $x_4$  are given for each atom. The contour lines for Cs, Sc, Si, O1, O2 and O3 are drawn with 2  $\text{e}\text{\AA}^{-3}$ , 1  $\text{e}\text{\AA}^{-3}$ , 5  $\text{e}\text{\AA}^{-3}$ , 0.5  $\text{e}\text{\AA}^{-3}$ , 0.2  $\text{e}\text{\AA}^{-3}$ , and 0.2  $\text{e}\text{\AA}^{-3}$ , respectively. Displacive modulation functions for each atom are given in Figures S9 – S14. In Figure S15 an additional selected section of the (3+1)-incommensurately modulated structure

highlights the infinite column of alternating [ScO<sub>6</sub>]-octahedra and six-membered [Si<sub>6</sub>O<sub>18</sub>]-rings along the  $\bar{3}$ -axis and the inter-column connection via a terminal oxygen atom. Figure S16 is a plot of Cs-O interatomic distances as a function of  $t$ . Figure S17 plots polyhedral microensembles found in Cs<sub>3</sub>ScSi<sub>6</sub>O<sub>15</sub>.

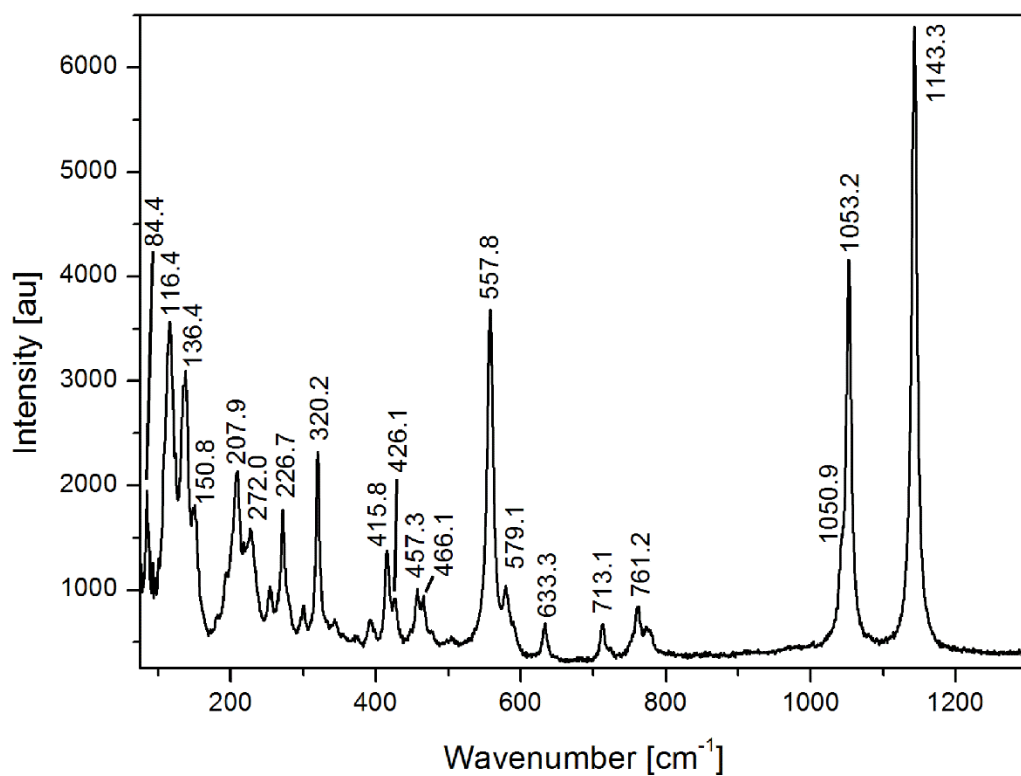


**Figure S1** Raman spectrum of Cs<sub>3</sub>ScSi<sub>6</sub>O<sub>15</sub>.

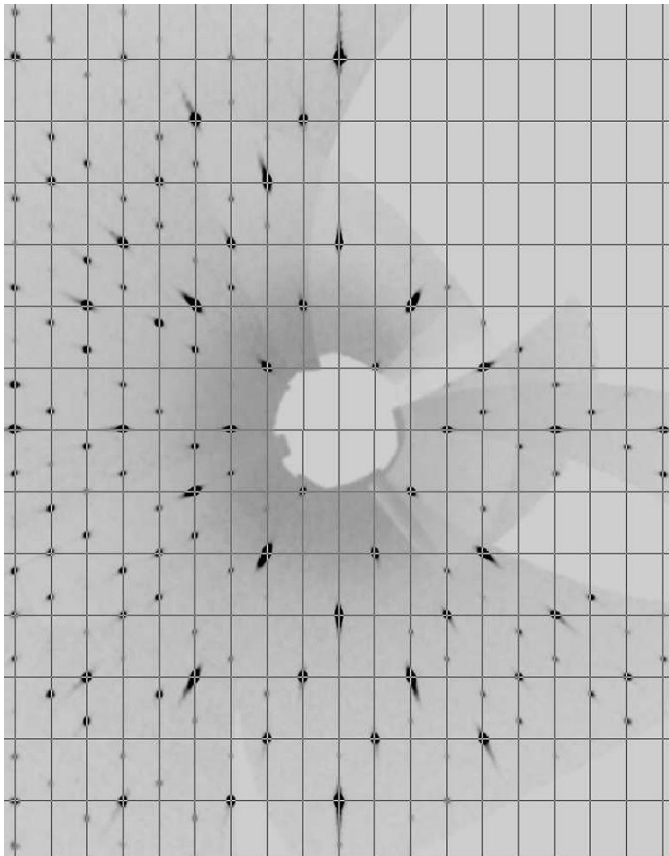


**Figure S2** Reconstruction of reciprocal space layer  $h0l$ ,  $a^*$  pointing to the left,  $c^*$  to the top.

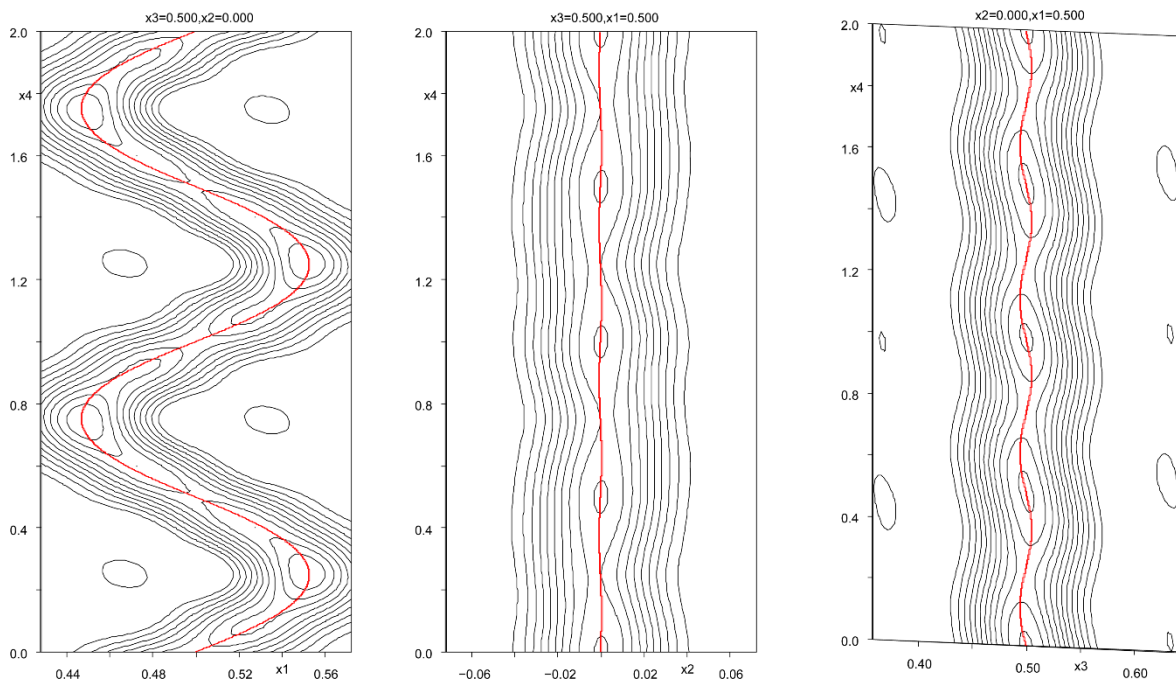


**Figure S3** Electron density sections for Cs.

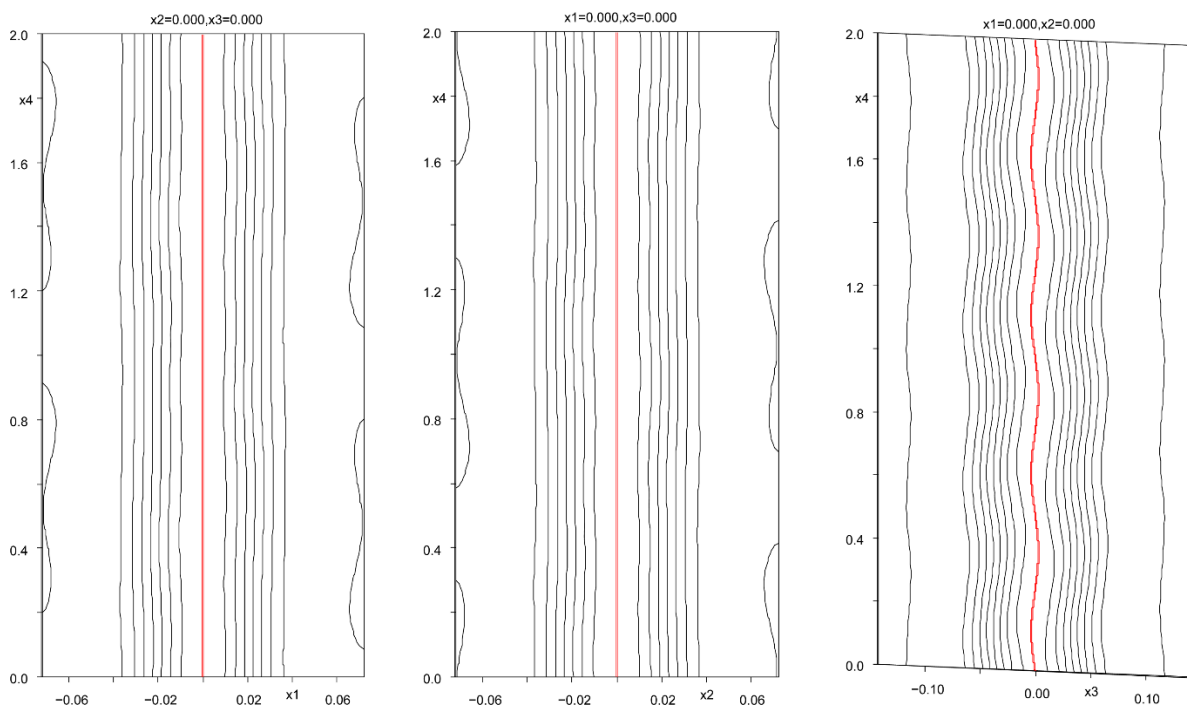


**Figure S4** Electron density sections for Sc.

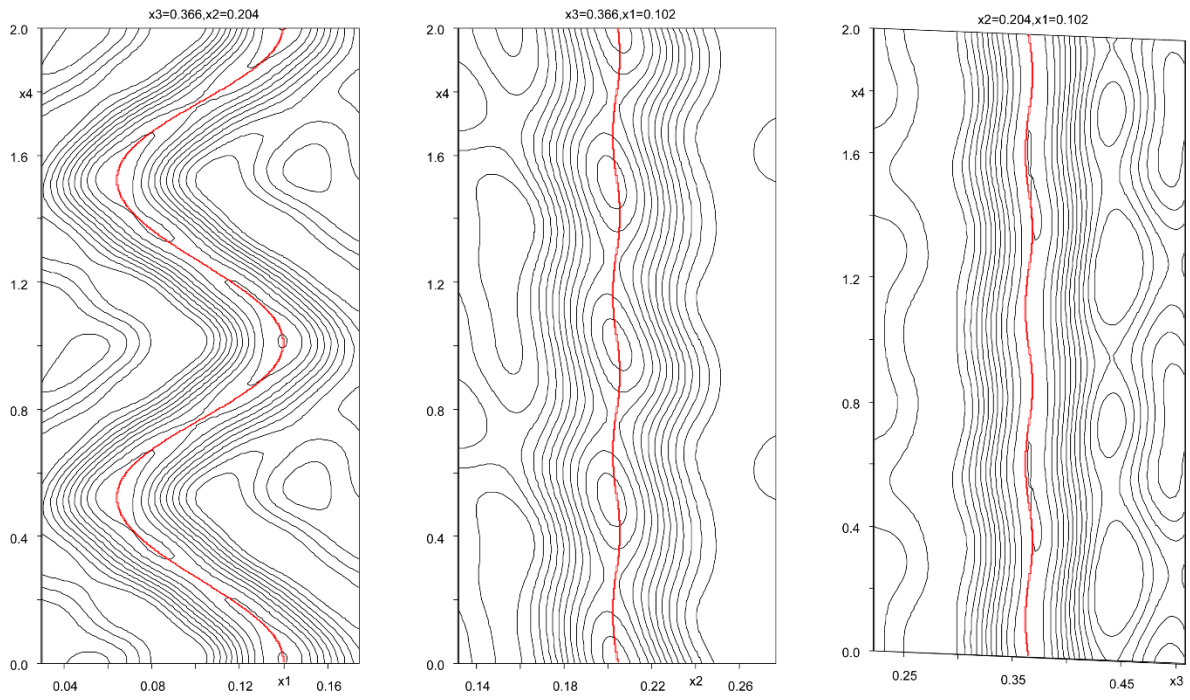


**Figure S5** Electron density sections for Si.

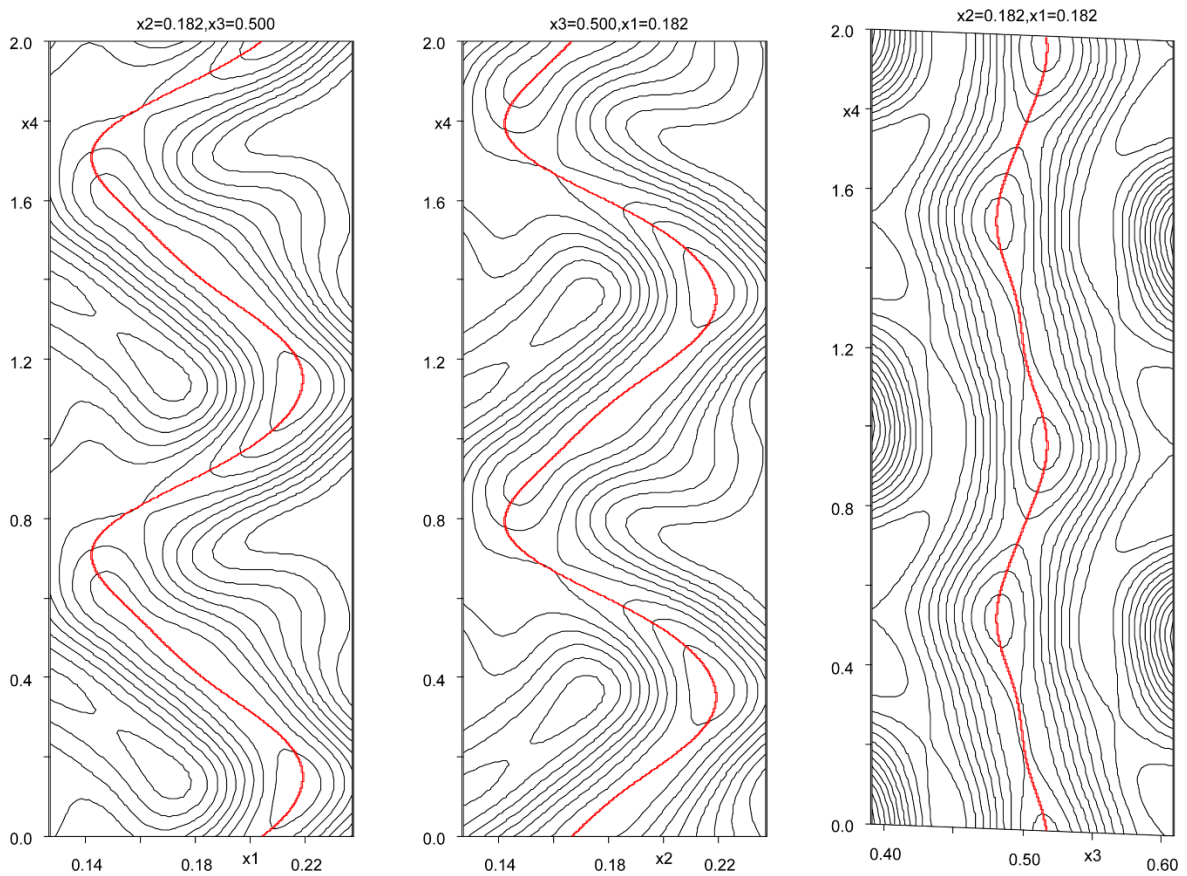


**Figure S6** Electron density sections for O1.

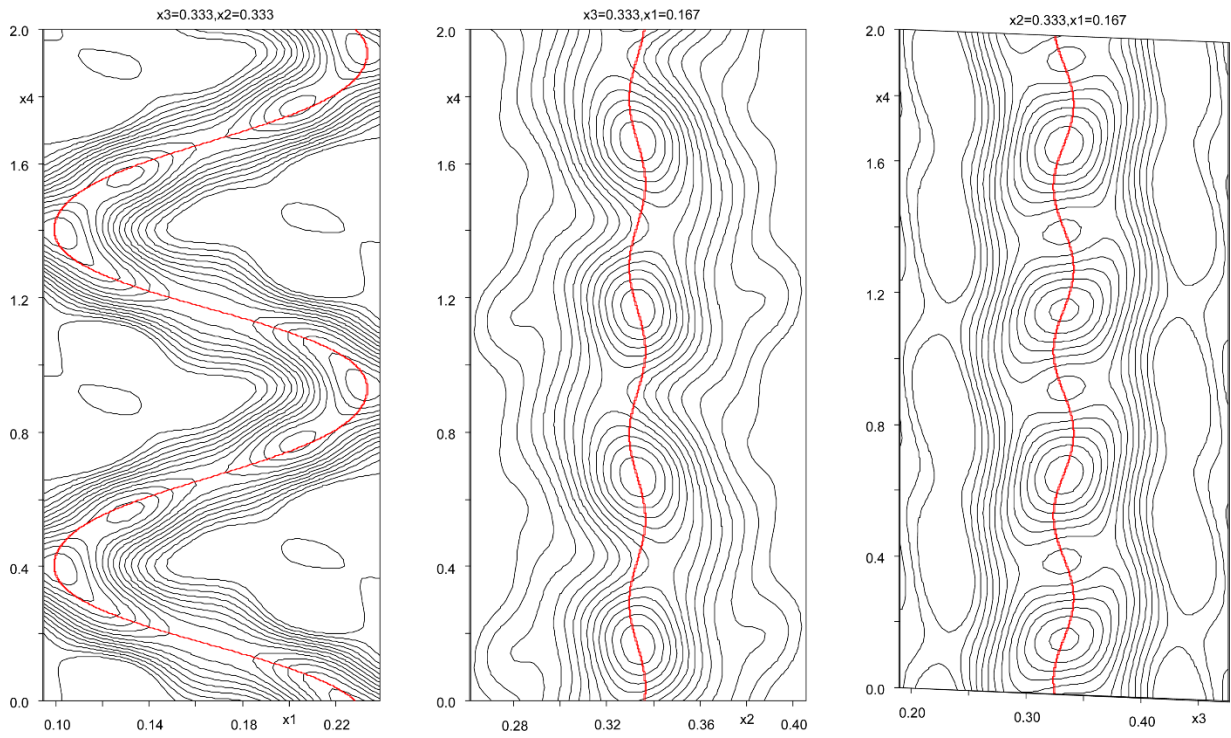


**Figure S7** Electron density sections for O2.

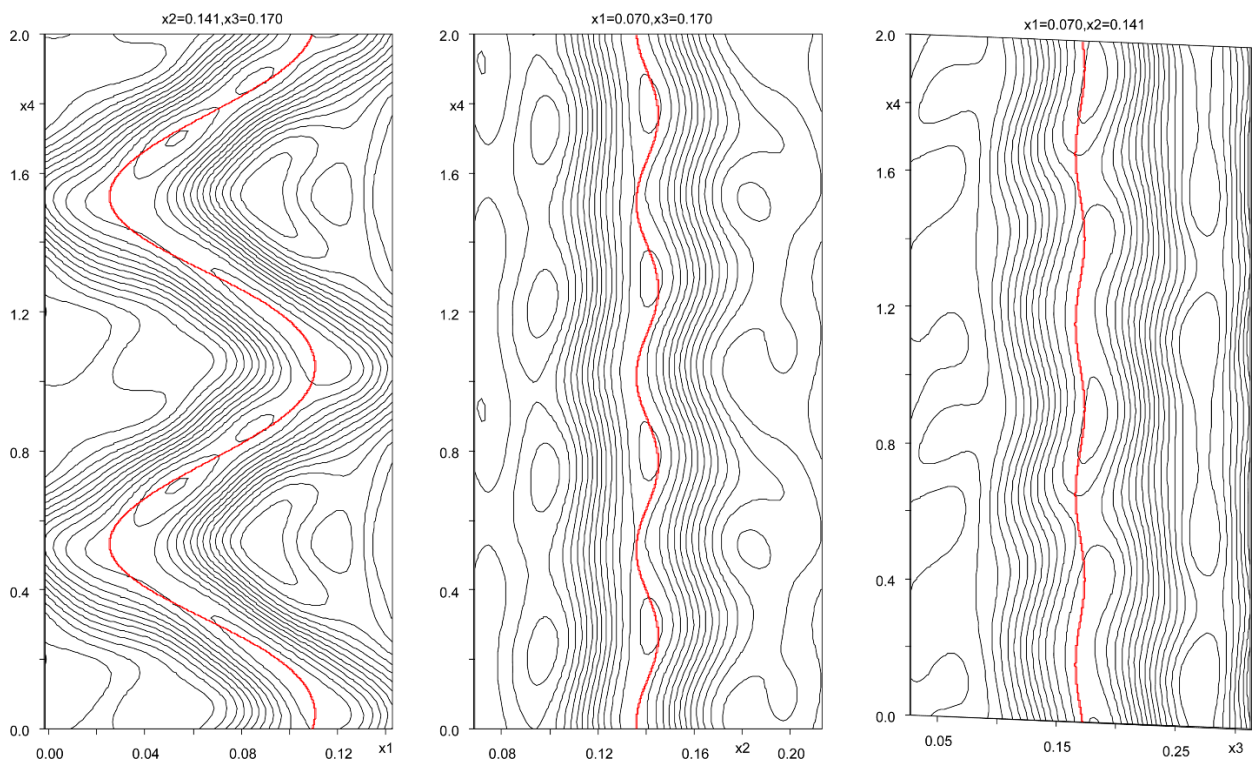


**Figure S8** Electron density sections for O3.



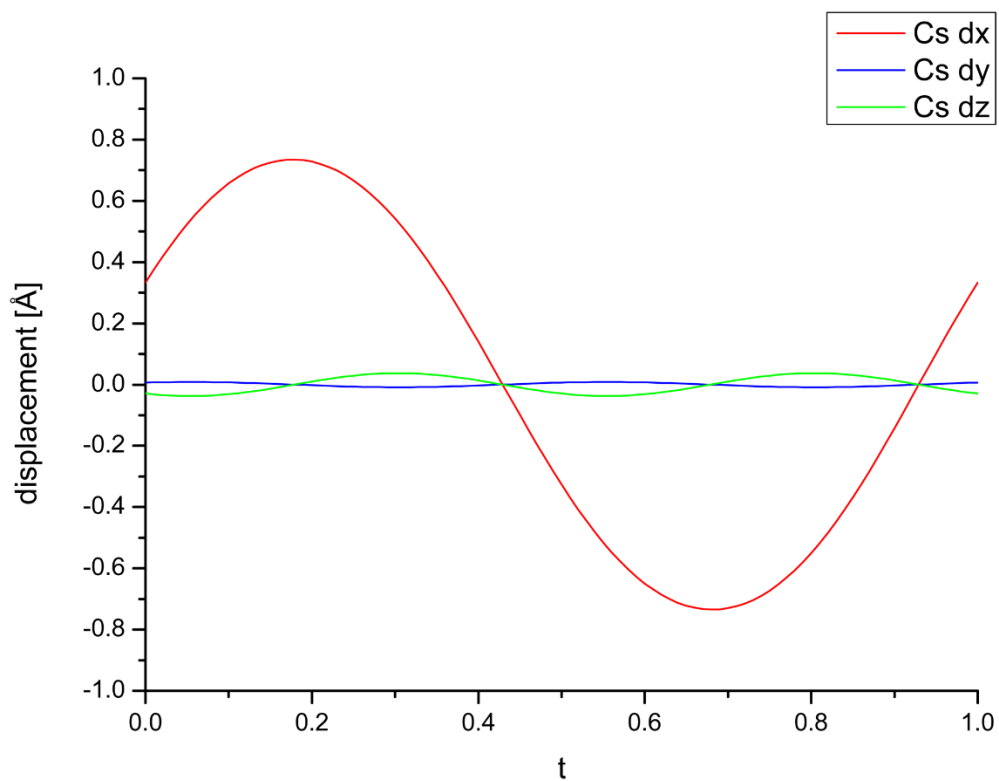


**Figure S9** Displacements of Cs.

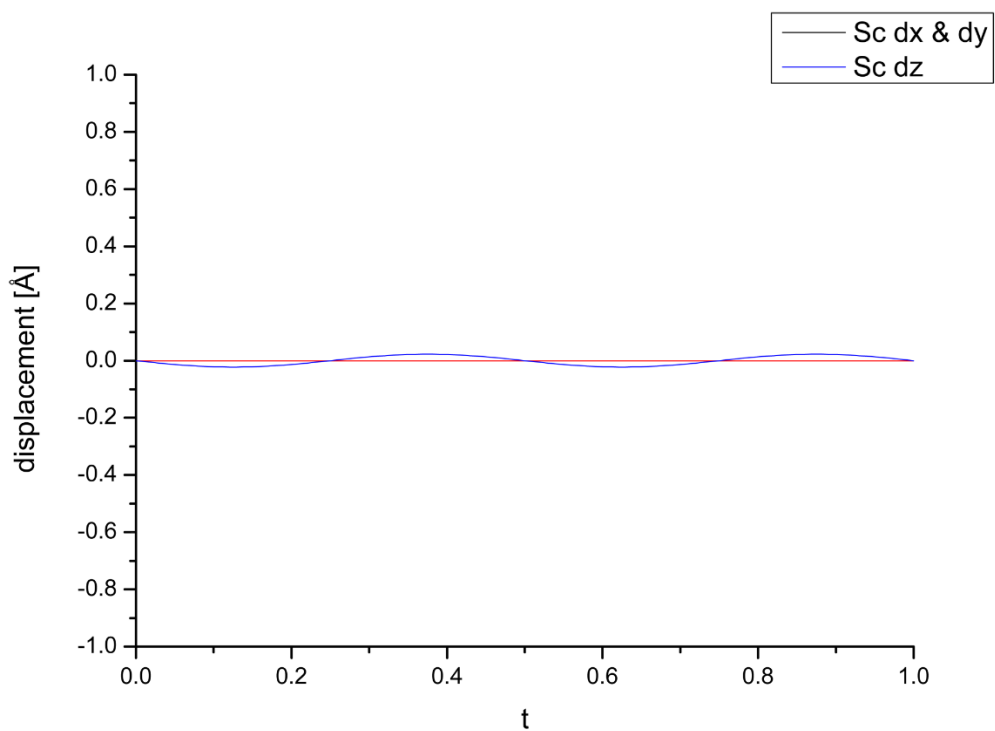


**Figure S10** Displacements of Sc.

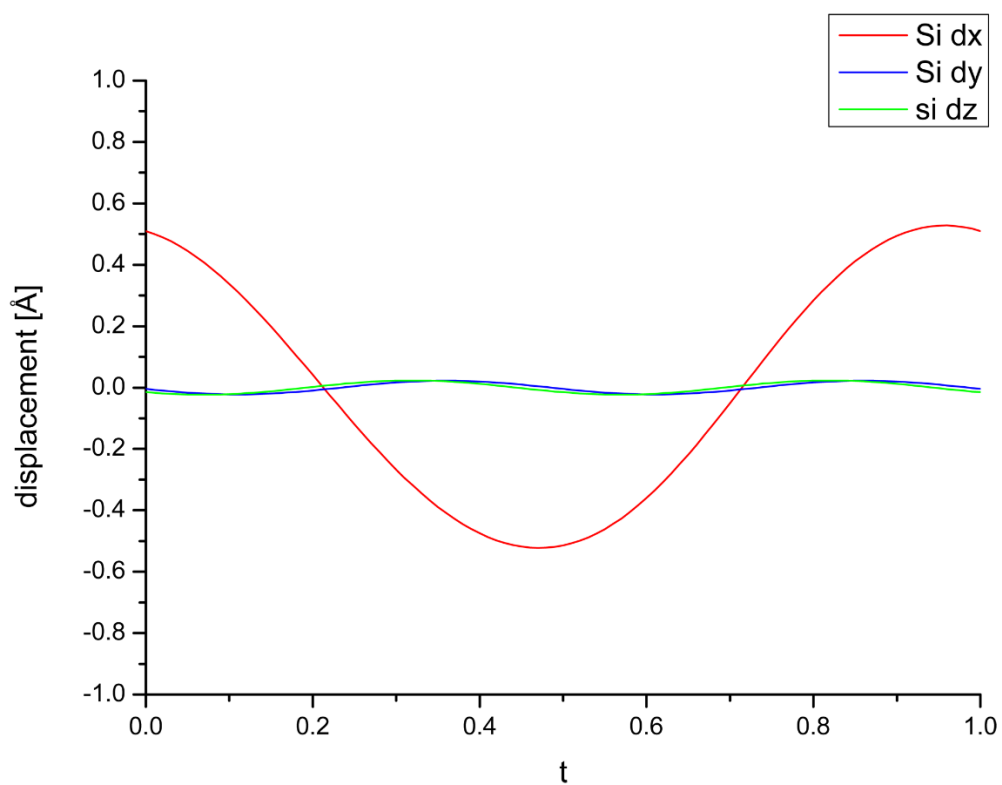


**Figure S11** Displacements of Si.

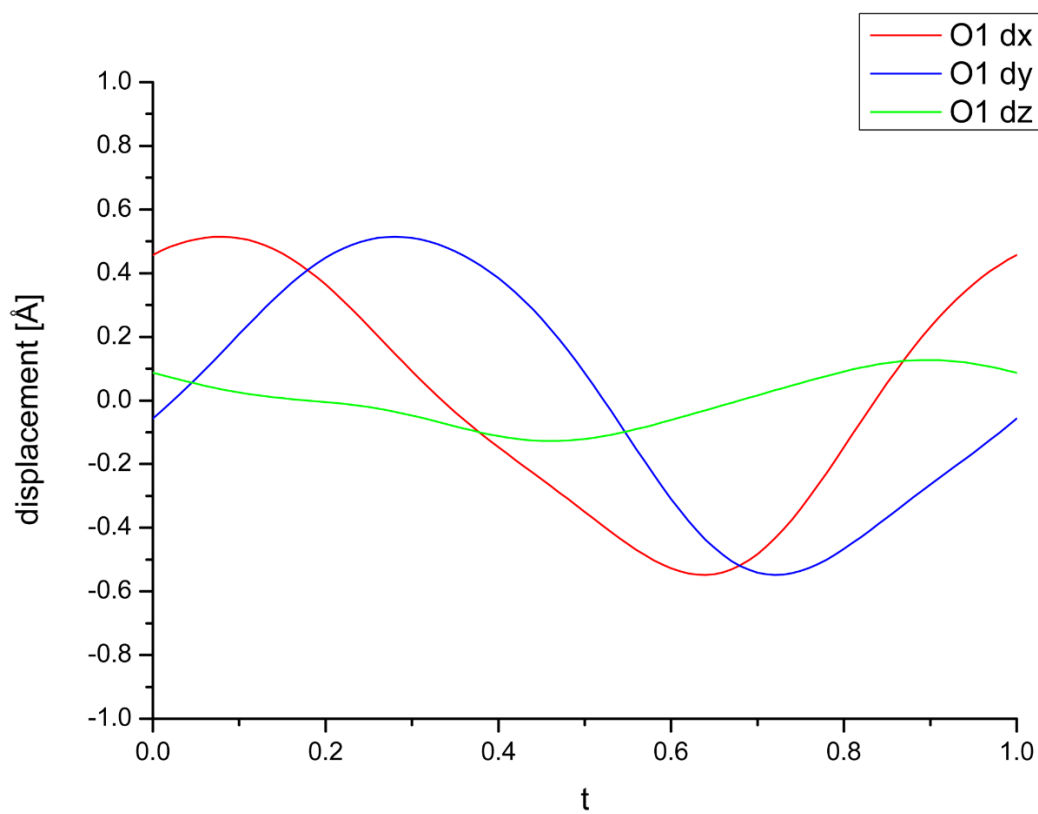


**Figure S12** Displacements of O1.

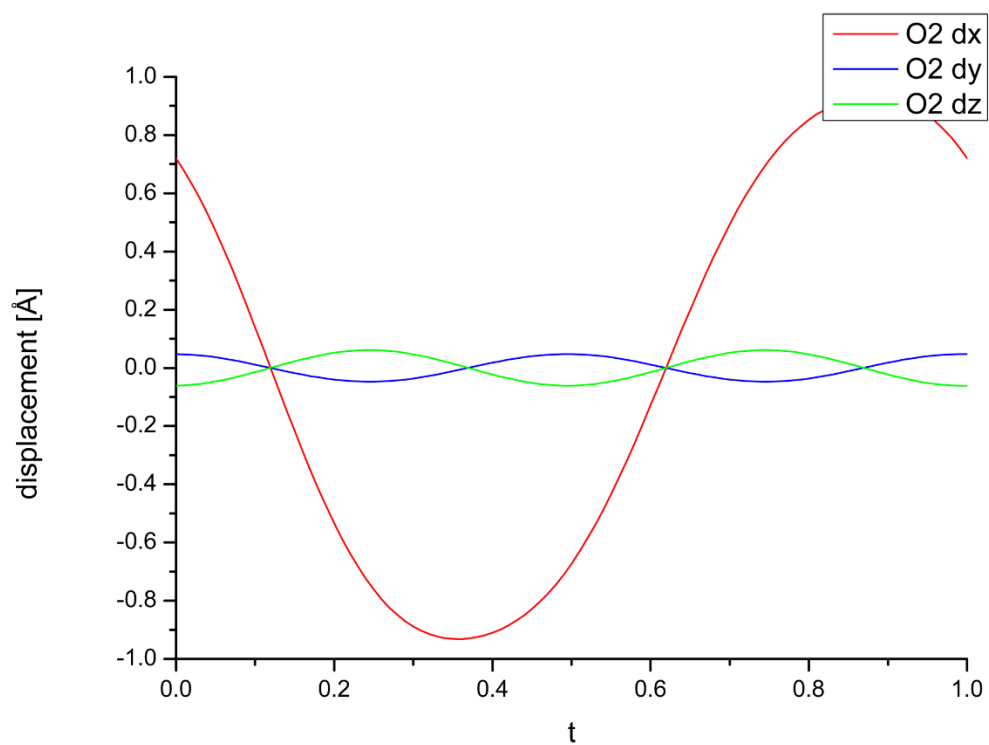


**Figure S13** Displacements of O2.

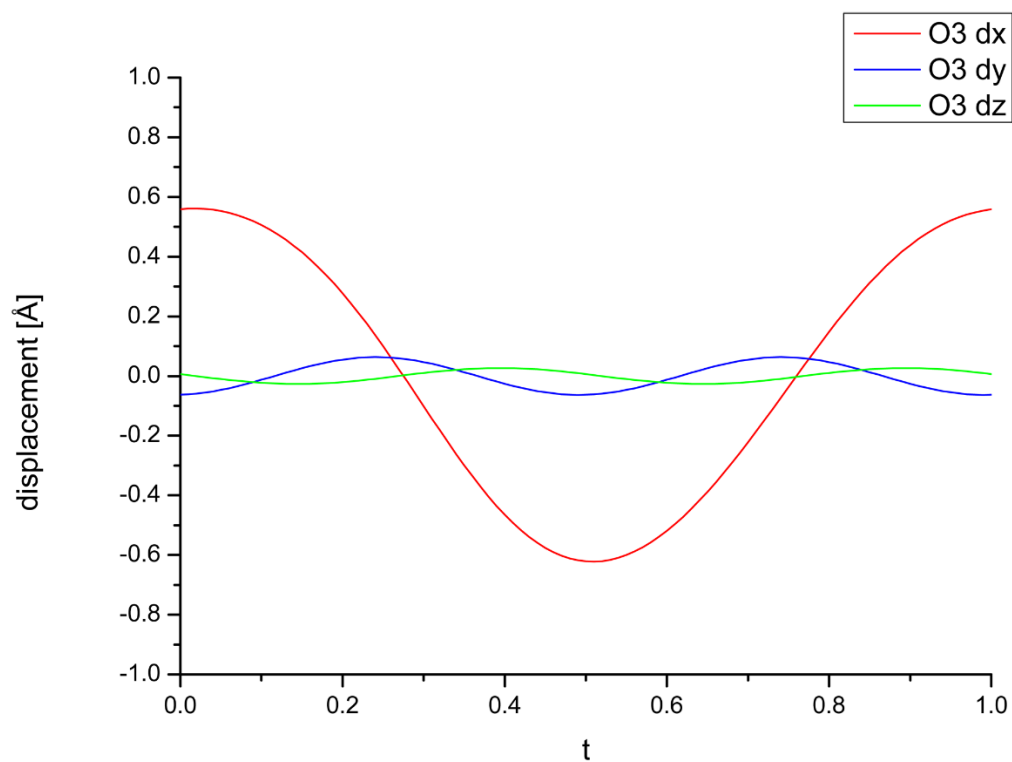


**Figure S14** Displacements of O3.

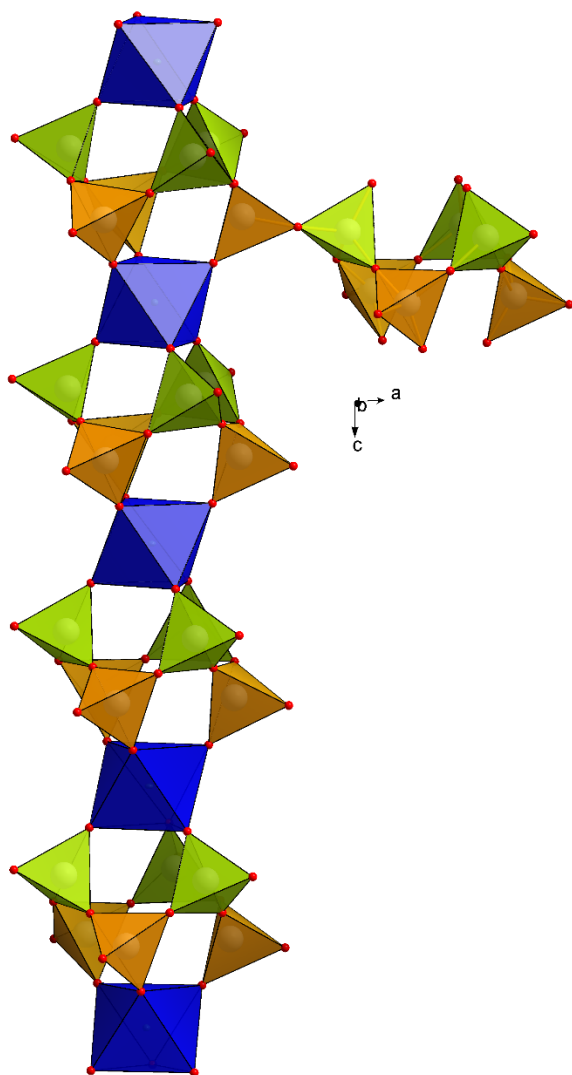


**Figure S15** A section of the infinite column of alternating  $[\text{ScO}_6]$ -octahedra and six-membered  $[\text{Si}_6\text{O}_{18}]$ -rings along the  $\bar{3}$ -axis in the (3+1)-incommensurately modulated structure of  $\text{Cs}_3\text{ScSi}_6\text{O}_{15}$ . Each  $[\text{ScO}_6]$ -octahedron is rotated relative to its adjacent  $[\text{ScO}_6]$ -octahedron. Notice, that the selected part of the modulated structure does not repeat translationally.

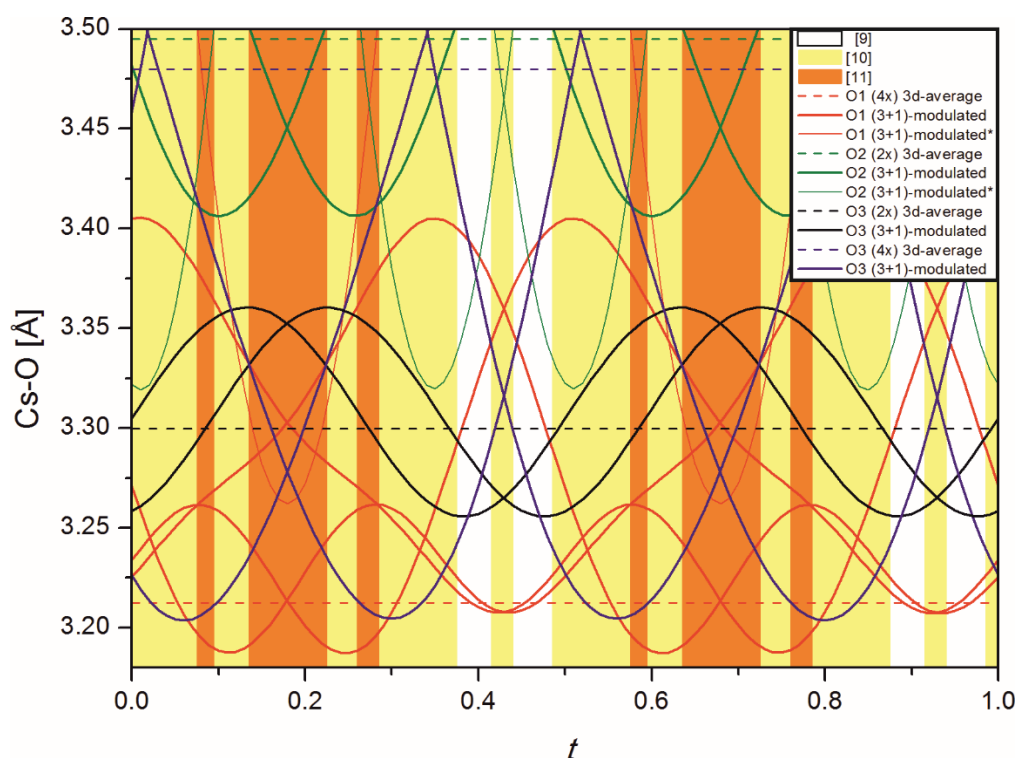


**Figure S16** Cs-O distances as a function of  $t$ . Cs-O distances that are symmetrically equivalent in the average structure diversify in the modulated structure for different values of  $t$ ; e.g. 4x Cs-O1 (broken red line) has an interatomic distance of 3.212(1) Å in the average structure whereas the corresponding interatomic distances in the modulated structure (think solid red line) ranging from 3.187(5) – 3.405(5) are represented by four individual lines. Thin solid lines represent interatomic Cs-O distances in the (3+1)-dimensionally modulated structure that correspond to a non-bonding distance in the average structure, i.e. distances that are larger than 3.5 Å in the 3d-average structure. The underlying background colour indicates the number of coordinating oxygen atoms in the modulated structure; white for nine-fold coordination, yellow for ten-fold coordination and orange for eleven-fold coordination.

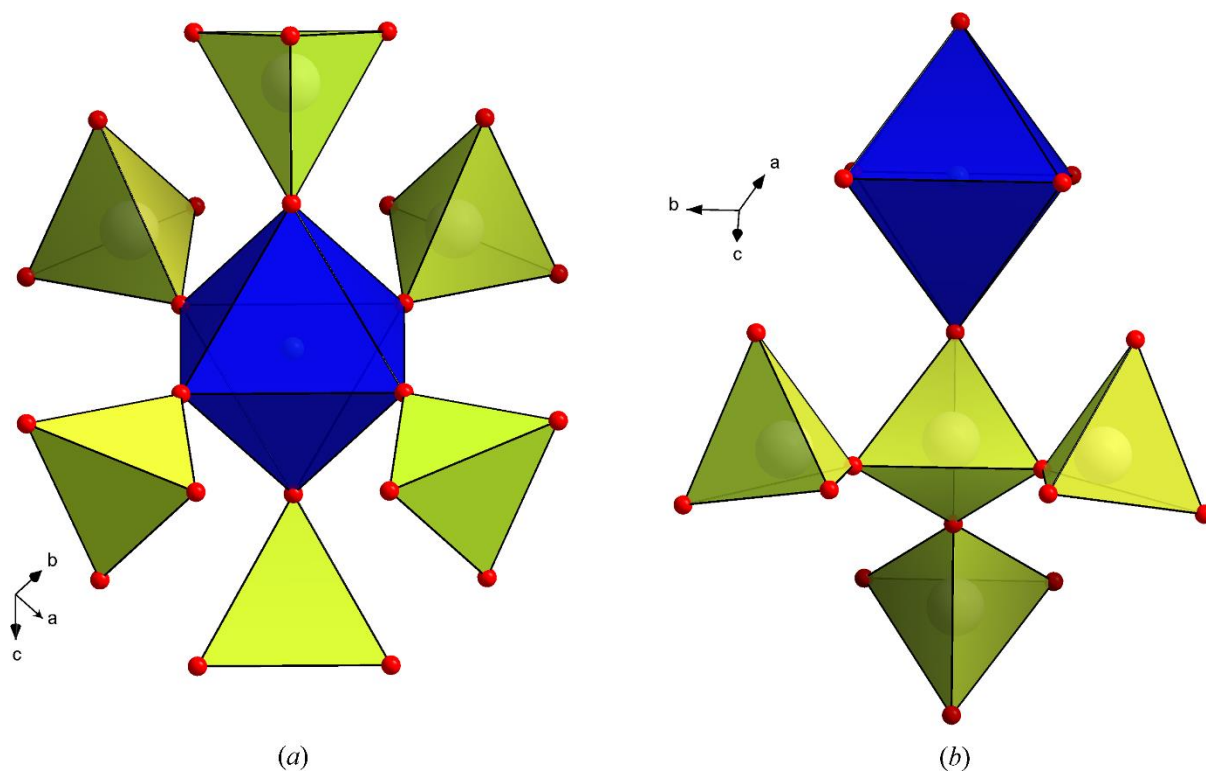


**Figure S17** Polyhedral microensembles (*PME*) of (a) the [ScO<sub>6</sub>]-octahedron (left) and (b) the [SiO<sub>4</sub>]-tetrahedron (right).